Local probing of arrested kinetics in Gd_5Ge_4

2008 J. Phys.: Condens. Matter 20 465212

(http://iopscience.iop.org/0953-8984/20/46/465212)

J. Phys.: Condens. Matter **20** (2008) 465212 (6pp) doi:10.1088/0953-8984/20/46/465212

Local probing of arrested kinetics in Gd_5Ge_4

J D Moore[1], G K Perkins[1], K Morrison[1], L Ghivelder[2], M K Chattopadhyay[3], S B Roy[3], P Chaddah[3], K A Gschneidner Jr[4], V K Pecharsky[4] and L F Cohen[1]

[1] The Blackett Laboratory, Imperial College London, London SW7 2AZ, UK
[2] Instituto de Física, Universidade Federal do Rio de Janeiro, C P 68528, Rio de Janeiro, RJ 21941-972, Brazil
[3] Magnetic and Superconducting Materials Section, Raja Ramanna Centre for Advanced Technology, Indore 452 013, India
[4] Ames Laboratory and Department of Materials Science and Engineering, Iowa State University, Ames, IA 50011-3020, USA

Received 6 June 2008, in final form 26 September 2008
Published 21 October 2008
Online at stacks.iop.org/JPhysCM/20/465212

Abstract
We present spatially localized magnetic relaxation measurements of the first-order magnetostructural transition in Gd_5Ge_4 using a scanning Hall probe imaging technique. Relaxation measurements were performed at 6, 10 and 35 K to probe the field-increasing antiferromagnetic (AFM) to ferromagnetic (FM) transition and, when it can occur, the field-decreasing FM to AFM transition. We demonstrate that localized regions relax with time towards the ground state for a given field and temperature and observe different magnetic behaviours at the three measurement temperatures. In particular, the observed magnetic relaxation at 6 K is consistent with the idea of an arrested state at this temperature. Our scanning Hall probe imaging data give an insight into the phase nucleation and growth process of the martensitic-like magnetostructural first-order transition in Gd_5Ge_4.

1. Introduction

Gd_5Ge_4 is the parent compound of the $Gd_5(Si_xGe_{1-x})_4$ family that displays giant magnetocaloric effect, giant magnetoresistance, colossal magnetostriction, and other interesting phenomena due to a first-order magnetostructural transition [1–3]. The germanide orders antiferromagnetically (AFM) below the Néel temperature ($T_N \cong 130$ K) in zero magnetic field with a Sm_5Ge_4-type orthorhombic layered structure. With the application of a magnetic field it undergoes a first-order transition to a ferromagnetic (FM) state that coincides with a structural transformation to a Gd_5Si_4-type orthorhombic structure [4].

The transition is characterized by the coexistence of the magnetic phases over certain field and temperature ranges [3, 5] and marked magnetic hysteresis in field and temperature. The precise magnetic state of the system that is reached depends on the magnetic and thermal histories. The spatial distribution of the phase coexistence in the global sample is on the micrometre length scale, which evolves via a nucleation and growth process as has been shown previously [6]. The microstructure can play an important role in the nucleation of one phase from the matrix of the other particularly when there are randomly oriented crystallites and a significant magneto-crystalline anisotropy [7]. Furthermore, the internal strain field that results from the large ∼1.1% volume change across the transition [4, 8–10] can randomize the transition behaviour.

An additional aspect of the Gd_5Ge_4 material is its behaviour at low temperatures in the so-called 'arrested state' ($T < 20$ K). The dynamics of the AFM to FM transition is kinetically arrested below 20 K and as a result in a zero applied magnetic field the material cannot reach its ground state which appears to be ferromagnetic [11, 12]. Instead it forms a glassy state consisting of a metastable (unconverted) AFM matrix along with a distribution of microscopic FM (equilibrium) regions [13]. The dynamics of this arrested state is similar to that observed in structural glasses [14, 15]. The arrest is partial between 10 and 20 K, and becomes complete below 10 K. Based on these observations, a revised H–T phase diagram was recently proposed [11, 12]. Using a spatially localized probe we have shown that both states coexist, the details

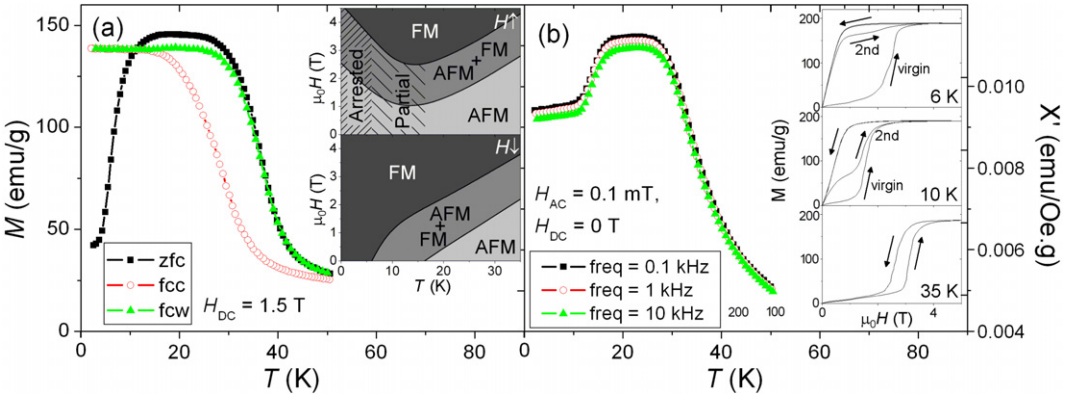

Figure 1. (a) M versus T plots in ZFC, FCC and FCW modes for applied magnetic field 1.5 T. The inset shows a schematic of the H–T phase diagram for increasing magnetic field (top) and decreasing magnetic field (bottom) see the text for a description of different regions. (b) AC susceptibility versus T for a change in frequency in zero applied magnetic field. The inset here shows isothermal M–H loops at 6, 10 and 35 K.

(This figure is in colour only in the electronic version)

again depend on magnetic history and sample morphology and magnetic anisotropy [6, 7]. We show here that the magnitude of the energy barrier between metastable phases varies on a spatially localized scale so that it is energetically favourable for regions of the material to switch to the magnetic glass ground state whilst other regions of the sample (distributed more or less isotropically through the sample) remain in the AFM state.

A general feature of the arrested state is the glass-like behaviour of magnetic relaxation, which is characterized by increasing relaxation times as the temperature is decreased. A similar behaviour was also reported for the manganese oxide compounds (La, Pr, Ca)MnO_3 [16, 17]. The dynamics across the transition was studied previously by global magnetization in polycrystalline [18] and single crystal [19] Gd_5Ge_4. These measurements show that the dynamics depends on the competition between magnetic, strain and thermal energies. In particular as might be expected, at high temperatures thermal activation facilitates excitation over the strain energy barriers, the system quickly approaches the equilibrium state and little magnetic relaxation is observed. At low temperatures, where the transition is arrested, the starting metastable state approaches equilibrium much more slowly and consequently significant magnetic relaxation is observed. In the present work we investigate details of the local behaviour of magnetic relaxation across the transition at 6, 10 and 35 K using Hall probe imaging. At the lowest temperature the magnetic glass state is realized over most of the sample but as temperature increases, more of the sample transforms into the AFM state as the magnetic field is cycled. At 35 K the AFM state is completely recovered when the magnetic field is cycled through the transition.

2. Experimental method

Scanning Hall probe images were taken on a $3 \times 3 \times 0.8$ mm^3 polished sample of polycrystalline Gd_5Ge_4 that has been studied in earlier works [6, 7]. The sample was prepared by arc-melting a mixture of Gd and Ge on a water cooled copper hearth in an argon atmosphere under ambient pressure [20, 21]. The as-cast alloy was quite brittle with a plate-like grain structure on the surface and inside the button. The material was studied in the as-cast condition without heat treatment after it was found to be single phase with the Sm_5Ge_4-type crystal structure by using x-ray powder diffraction and optical metallography.

Local magnetic Hall images were made using a custom-built scanning Hall probe microscope [22] that measures local magnetic induction with a 25×25 μm^2 InSb Hall probe. The Hall sensor was rastered in a plane 10 μm above the polished sample surface in constant magnetic field and temperature. This produces a two dimensional profile of the magnetization component perpendicular to the surface covering an area up to 4×4 mm^2 (128×128 pixel) with pixel resolution of 30×30 μm^2. Images took approximately nine minutes each to complete, after which they were cropped to an area 1400×1400 μm^2 corresponding to a central region of the sample plane. The Hall probe apparatus and sample were inserted in an Oxford instruments double-axis transverse field magnetometer with the magnetic field applied perpendicular to the sample plane. Magnetization measurements were performed in an Oxford Instruments longitudinal vibrating sample magnetometer. The ac susceptibility was measured at different frequencies with a Quantum Design PPMS.

The sample was cooled in zero magnetic field from above T_N before reaching the measurement temperatures of 6, 10 and 35 K. The relaxation experiments involved taking 18 successive Hall images over a period of 156 min. The target H in the phase coexistence region was arrived at by either increasing H from zero when investigating the dynamics of the increasing field-leg or decreasing H from 4 T when investigating the dynamics of the decreasing field-leg and then immediately taking Hall images.

3. Results

Figure 1(a) shows magnetization versus temperature curves in 1.5 T applied magnetic field for zero field cooled (ZFC),

field cooled cooling (FCC) and field cooled warming (FCW) modes. The different paths followed by the ZFC and FCW curves below 20 K highlights extent of the arrested state while above this temperature the paths join and the sample shows the more usual first-order phase transition behaviour. The inset to figure 1 is a schematic of the H–T phase diagram of the sample below 35 K for the field-increasing AFM to FM transition (top plot) and the field-decreasing FM to AFM transition (bottom plot). The AFM/FM phase coexistence region has been shaded medium-grey. The regions of the phase diagram where the sample is fully arrested and where only some fraction of the sample volume becomes arrested are indicated in the top of these two plots.

Figure 1(b) shows magnetic susceptibility versus temperature in zero applied DC magnetic field for an AC magnetic field amplitude 1 Oe and frequencies of 0.1, 1 and 10 kHz. There is a broad peak in the susceptibility consistent with the magnetic glass picture, and the frequency dependence continues well above the peak temperature (10 K). Additionally the peak hardly shifts with change in frequency so it is immediately clear that the low temperature state is not associated with a spin glass [23]. The inset to figure 1(b) shows isothermal M–H loops at the temperatures 6, 10 and 35 K to illustrate the different global magnetic behaviour that is observed. By comparing the second increasing field-leg with the virgin field-leg it is clear the sample volume is mostly in the arrested FM state at 6 K, partially in the arrested state at 10 K and outside the arrested region at 35 K. Although the FM phase appears to be the ground state at 6 K, the conversion of FM to AFM phase on the downwards field-leg can be explained from the rough landscape picture of a disorder broadened first-order phase transition. In this picture for this sample at this temperature there are pockets where the FM to AFM transition is not arrested such that the return transformation is possible.

Having illustrated the reversible and arrested magnetic behaviour at the temperatures of interest in the phase diagram, we now present in figure 2 the Hall imaging results of magnetic relaxation at 6 K. In images (a)–(c) the sample is ZFC to 6 K and then a field 1.6 T is applied. (The different applied field values at 6, 10 and 35 K correspond to points just above the onset of the transition (i.e., approximately 25% AFM and 75% FM phase fractions), except at 6 K and 0.5 T on the $H\downarrow$ field-leg where the FM–AFM transition is arrested) Likewise in (d)–(f) the field is reduced from 4 T, well within the FM state, to 0.5 T where we investigate the field-decreasing ($H\downarrow$) transition. To be concise we show only the first Hall images, (a) and (d), and the last images, (b) and (e) in each set of 18. The Hall images are displayed with a black to white contrast scale where black represents regions of low induction and white represents regions of high induction. In Gd_5Ge_4 the FM magnetization is much larger than the AFM magnetization (see inset in figure 1(b)) so it is safe associate black regions with the AFM phase and white regions with the FM phase. We highlight the changes between the first and last Hall images by subtracting one from the other and have labelled the result the 'difference' image in (c) and (f). Regions in the difference images that have changed or relaxed are coloured white and regions that have remained unchanged

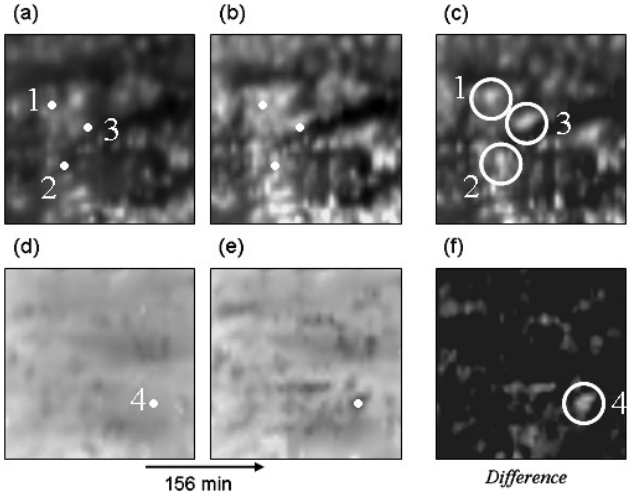

Figure 2. Scanning Hall probe images at 6 K recorded on the $H\uparrow$ field-leg at $H = 1.6$ T ((a)–(c)) and on the $H\downarrow$ field-leg at $H = 0.5$ T ((d)–(f)). The initial images are (a) and (d) and the final images 156 min later are (b) and (e). Hall images represent a central region 1400×1400 μm^2 of the sample where black corresponds to the AFM phase and white to the FM phase. Parts (c) and (f) show the respective difference images, i.e., the magnetization change between the first and last Hall images. (Black represents regions that have remained unchanged and white represents regions that have undergone magnetic relaxation.)

are shown as black. Inspection of the difference image on the $H\uparrow$ field-leg (figure 1(c)) shows that many discrete regions distributed over the whole window have switched and that these are about 50–300 μm in size. In contrast, on the $H\downarrow$ field-leg (figure 1(f)) only a few regions have switched phase. We shall discuss this point later in terms of the low temperature glass state in Gd_5Ge_4.

A few of the regions that have switched in the difference images in figures 2(c) and (f) are identified by the white circles and numeric labels. At these locations, the magnetization versus time (t) has been extracted from a single pixel. The $M(t)$ curves normalized with respect to the initial magnetization M_0 for the numbered locations in figure 2 are plotted in figure 3(a) on the $H\uparrow$ field-leg and figure 3(b) on the $H\downarrow$ field-leg. The corresponding global magnetization curves computed by integrating over the entire image are shown for comparison. We chose pixel locations that best illustrate the different magnetic relaxation behaviour seen over the image window. In figure 3(a), curves 1–3 show regions that have relaxed with time from the metastable AFM state to the FM ground state. The local $M(t)$ curves are stochastic and they relax gradually towards some constant M value with times varying from 35 min for curve-1 to over 156 min for curve-3. Curve-4 in figure 3(b) shows the reverse process on the $H\downarrow$ field-leg where a region relaxes from the FM state to the AFM state. The transition is again gradual taking nearly 50 min to complete but it was triggered only after 46 min had passed, highlighting the stochastic nature of the relaxation process.

Next we compare the global $M(t)$ curve from the magnetic intensity over the whole image window using a deconvolution procedure [24]. The global curves are shown by the closed

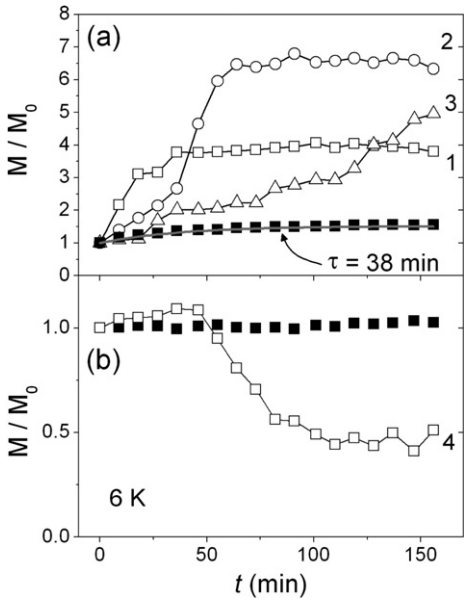

Figure 3. Magnetization versus time plots $M(t)$ at 6 K on (a) the $H\uparrow$ field-leg at $H = 1.6$ T and (b) the $H\downarrow$ field-leg at $H = 0.5$ T. The global magnetization (closed symbols) and local magnetization (open symbols) are extracted from the 18 consecutive Hall images. The numbers correspond to marked locations in Hall images in figure 2.

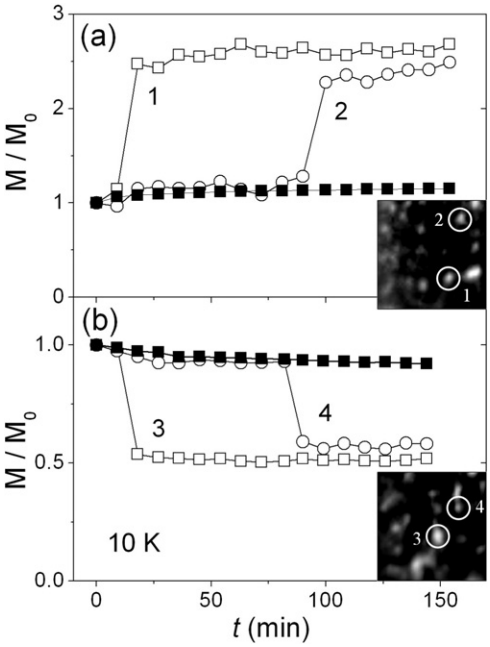

Figure 4. Magnetization versus time plots $M(t)$ at 10 K on (a) the $H\uparrow$ field-leg at $H = 1.4$ T and (b) the $H\downarrow$ field-leg at $H = 0.7$ T. The global magnetization (closed symbols) and local magnetization (open symbols) are extracted from the 18 consecutive Hall images. The insets are the difference Hall images obtained from subtracting the initial and final (156 min later) images. Black represents regions that have remained unchanged and white represents regions that have undergone magnetic relaxation. Locations of the local $M(t)$ curves are numbered in the inset images.

square symbols in figures 3(a) and (b) and are also normalized with respect to the initial magnetization M_0. In figure 3(a) the global $M(t)$ on the $H\uparrow$ field-leg shows significant magnetic relaxation of approximately 1.6 times of M_0 and can be described well by the exponential form $M/M_0 \propto \exp(-t/\tau)$ with a characteristic relaxation time $\tau \sim 38$ min. In contrast, the global $M(t)$ curve on the $H\downarrow$ field-leg in figure 3(b) suggests that no measurable relaxation has taken place over the experimental period in agreement with the FM state being the ground state. However the local $M(t)$ curve no. 4 in the same figure reveals that a small region had indeed relaxed. As mentioned previously, from the rough landscape picture there are regions of the sample volume that have energy barriers low enough for this to happen although at this temperature these regions are a very small fraction of the overall energy landscape.

In a similar fashion to the relaxation imaging presented in figures 2 and 3 at 6 K, we now show data at 10 K in figure 4 for local and global $M(t)$ curves on (a) the $H\uparrow$ field-leg at $H = 1.4$ T and on (b) the $H\downarrow$ field-leg at $H = 0.7$ T. For brevity, the insets to figures 4(a) and (b) show only the difference images and the numbered locations 1–4 where the local $M(t)$ curves were taken. The difference images highlight that many localized regions have switched phase on both field-leg directions. At this temperature the formation of the glass state is known to be only partial but a proper representation of the spatial variation has not been previously appreciated. The density of sites where relaxation can occur from the FM glass to the AFM state (figure 4(b)) is significantly higher at this temperature than at 6 K (see figure 2(f)). The local $M(t)$ curves show that regions switch sharply with a distinct step in the magnetization, thus providing a microscopic illustration of earlier reported avalanche-like behaviour in Gd_5Ge_4 [18, 25]. This behaviour is different from the slow local relaxation dynamics observed at 6 K. However, both temperatures show the same qualitative behaviour on both the $H\uparrow$ and $H\downarrow$ field-legs so the relaxation process is the same for transitions from metastable AFM to ground state FM and from FM to supercooled AFM. Again the local transitions occur at random times throughout the experiment timescale. The global $M(t)$ curve on the $H\uparrow$ field-leg (figure 4(a)) showed a magnetization change of $\sim$1.15 times from M_0 which is less than at 6 K as at this temperature (10 K) the system has moved into the only partially arrested state. Likewise, the global $M(t)$ curve on the $H\downarrow$ field-leg (figure 4(b)) showed magnetization change of $\sim$0.9 times M_0 which reflects more regions becoming unblocked from the arrested state at 10 K than at 6 K that are now able to undergo transition from FM to AFM.

In figure 5 we show relaxation imaging results at 35 K. Part (a) shows global and local $M(t)$ curves on the $H\uparrow$ field-leg at $H = 3.3$ T and part (b) on the $H\downarrow$ field-leg at $H = 2.9$ T. The difference Hall images for each field direction are shown in the insets along with the two locations marked for the local $M(t)$ curves. The local transitions from AFM to FM and from FM to AFM show sharp steps similar to the behaviour at 10 K. The main difference is that both global $M(t)$ curves in figures 5(a) and (b) show considerably less magnetic relaxation has taken place at 35 K when compared to the 6 and 10 K global curves. We repeated Hall imaging of relaxation at 35 K

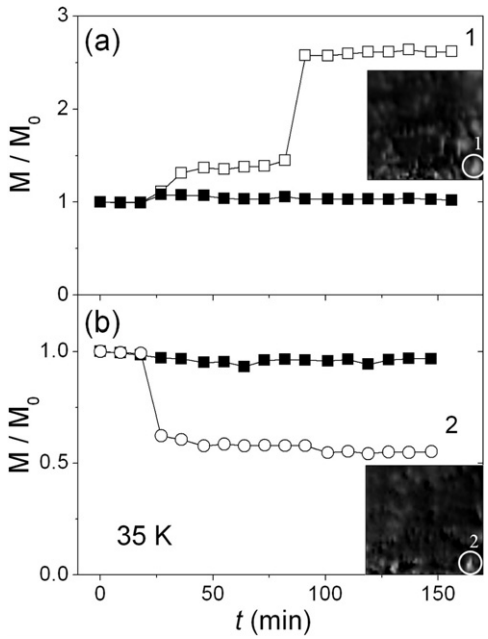

Figure 5. Magnetization versus time plots $M(t)$ at 10 K on (a) the $H\uparrow$ field-leg at $H = 3.3$ T and (b) the $H\downarrow$ field-leg at $H = 2.9$ T. The insets are the difference Hall images. The global $M(t)$ are closed symbols and local $M(t)$ are open symbols.

at the slightly lower applied magnetic fields of $H\uparrow = 2.9$ T and $H\downarrow = 2.4$ T which correspond to a lower point in the phase coexistence region of the H–T diagram and obtained similar quantitative results.

4. Discussion

Here we discuss behaviour of the magnetic relaxation at 6, 10 and 35 K shown in figures 2–5 and remark on two main observations from the imaging data. The first point is the degree of relaxation observed at each temperature and second is the different behaviour between local and global $M(t)$ curves.

At 6 K the global $M(t)$ curve on the $H\downarrow$ field-leg (figure 3(b)) showed little or no relaxation which is expected at this temperature since the sample is well within the magnetic glass region. But we observe relaxation locally from the FM to AFM state so there are some regions in the rough disorder landscape where the energy barrier is low enough for this to occur even at this temperature. This is consistent with the x-ray powder diffraction findings in [4] where on about an hour-long experimental timescale, 93% of the sample volume transforms to the high-field crystal structure in a 4 T field at this temperature, but when the magnetic field is reduced to zero, the concentration of the high-field phase is lowered from 93 to 86 vol% in a similar polycrystalline Gd_5Ge_4 sample. On the $H\uparrow$ field-leg, a relatively large amount of relaxation from AFM to FM occurred as the FM state is stable here. Such large relaxation in a single crystal Gd_5Ge_4 was found by Roy *et al* [12] and was compared to the re-crystallization process of polymers [26] which occurs via a nucleation and growth process where it is the growth of crystallites that dominates the rapid volume fraction increase of the ground state. This picture is consistent with the local $M(t)$ relaxation curves at 6 K (figure 3) which show that switching is a continuous growth of one phase. The characteristic time for bulk relaxation at 6 K was ∼38 min which is of the order of that reported elsewhere [12, 19].

At 10 K the bulk $M(t)$ curves (figure 4) reveal magnetic relaxation of approximately 10–20% from the initial magnetization value M_0 for both the $H\uparrow$ and $H\downarrow$ field directions. Some regions of the sample are now unblocked from the arrested state and can undergo magnetic relaxation. Global relaxation at 6 and 10 K measured here is consistent with the reported bulk magnetization measurements [18, 19]. Moving on to the local relaxation behaviour at 10 K, the curves in figure 4 show sharp step-like changes in the magnetization, which contrast with the slower growth processes at 6 K. This change in local behaviour coincides with being at the higher temperature where the arrested state is only partially realized over the sample volume. At 35 K we are completely outside the glassy region of the phase diagram and we associate the sharp local behaviour with the metamagnetic transition. Similar relaxation behaviour was reported in single crystal Gd_5Ge_4 [19] where sharp magnetization steps were observed above 14 K and smoother changes in the magnetization at lower temperatures.

The role of microscopic nucleation and growth rates through the first-order field-driven AFM to FM transition in Gd_5Ge_4 was previously modelled by Perkins *et al* [27]. They found that the nucleation rate of the FM clusters in the AFM matrix was approximately an order of magnitude larger at 35 K than at 6 K and that the growth dynamics were similar at the two temperatures. The difference between that study and the present work is the fact that here we focus on relaxation rather than the dynamics of the field-driven nucleation and growth behaviour. Nevertheless there are two observations that show consistency between these two studies. (1) The fact that the nucleation rate is faster at 35 K in the field-driven case supports the idea that the energy barrier to move from one state to the other is effectively lower at this temperature. (2) The fact that at 6 K, slow growth of clusters dominates the transitional region in the field-driven transition and this is again consistent with present observations. Here we also see a slow relaxation process at 6 K, whereas at a higher temperature predominantly sharp nucleation events occur with time. Overall the $M(t)$ curves in figures 3–5 highlight the significantly different local and global magnetic behaviour in the magnetic relaxation process in Gd_5Ge_4, which is a point not directly inferred from previous bulk relaxation measurements [18, 19].

Indeed it is interesting to make direct comparison with field-driven isothermal $M(H)$ measurements. We see sharp local switching at high temperatures but with a range of onset fields. This translates to a broad $M(H)$ curve as the transition is crossed when measured globally. At low temperature we see slow local switching but the significant relaxation process implies that in this regime experimental observations will be highly dependent on the sweep rate of the magnetic field. This is entirely consistent with previous global observations showing that the sharpness of the transitional features in

the $M(H)$ curve is dependent on the external field ramp rate [19, 25].

5. Conclusion

In conclusion, we have used global magnetometry and AC susceptibility to map out the phase diagram for the particular polycrystalline sample under study. We have imaged magnetic relaxation of the AFM $\leftrightarrow$ FM transition at 6 K in the magnetic glass state, at 10 K where some of the sample volume can undergo the FM–AFM transition and at 35 K where the FM–AFM is completed over the whole sample. We observed relaxation as the random switching of macroscopic clusters 30–300 μm in size over the image window in the 'difference' Hall images in figures 2, 4 and 5. The magnetic behaviour switches from a slow growth process at 6 K characteristic for a glassy transition to a sharper, nucleation dominated process at 10 K and higher temperatures. The amount of global relaxation is in agreement with the state at 6 K being the magnetic glass and the state at 10 K being partially arrested, while the little relaxation observed at 35 K means the metastable state that is reached upon sweeping to a given field is close to the equilibrium state.

Acknowledgments

Work at Imperial College is supported by EPSRC EP/E016243/1 and the Leverhulme Trust. Work at the Ames Laboratory is supported by the US Department of Energy, Office of Basic Energy Sciences, Materials Sciences Division under contract No. DE-AC02-07CH11358 with Iowa State University of Science and Technology.

References

[1] Pecharsky V K and Gschneidner K A 1997 *Phys. Rev. Lett.* **78** 4494
[2] Levin E M, Pecharsky V K and Gschneidner K A 1999 *Phys. Rev.* B **60** 7993
[3] Magen C *et al* 2003 *J. Phys.: Condens. Matter* **15** 2389
[4] Pecharsky V K, Holm A P, Gschneidner K A and Rink R 2003 *Phys. Rev. Lett.* **91** 197204
[5] Pecharsky V K and Gschneidner K A 2007 *Pure Appl. Chem.* **79** 1383
[6] Moore J D *et al* 2006 *Phys. Rev.* B **73** 144426
[7] Moore J D *et al* 2006 *Appl. Phys. Lett.* **88** 072501
[8] Ahn K H, Lookman T and Bishop A R 2004 *Nature* **428** 401
[9] Burgy J, Moreo A and Dagotto E 2004 *Phys. Rev. Lett.* **92** 097202
[10] Das A K *et al* 2003 *Phys. Rev. Lett.* **91** 087203
[11] Roy S B *et al* 2006 *Phys. Rev.* B **74** 012403
[12] Roy S B *et al* 2007 *Phys. Rev.* B **75** 184410
[13] Ouyang Z W *et al* 2006 *Phys. Rev.* B **74** 094404
[14] Brawer S 1985 *Relaxation in Viscous Liquids and Glasses* (Columbus, OH: The American Ceramic Society)
[15] Debenedetti P G and Stillinger F H 2001 *Nature* **410** 259
[16] Ghivelder L and Parisi F 2005 *Phys. Rev.* B **71** 184425
[17] Wu W D *et al* 2006 *Nat. Mater.* **5** 881
[18] Chattopadhyay M K *et al* 2004 *Phys. Rev.* B **70** 214421
[19] Ouyang Z W *et al* 2007 *Phys. Rev.* B **76** 134406
[20] Levin E M, Gschneidner K A and Pecharsky V K 2002 *Phys. Rev.* B **65** 214427
[21] Pecharsky V K and Gschneider K A 1997 *J. Alloys Compounds* **260** 98
[22] Perkins G K *et al* 2001 *IEEE Trans. Appl. Supercond.* **11** 3186
[23] Tholence J L 1980 *Solid State Commun.* **35** 113
[24] Perkins G K, Bugoslavsky Y V and Caplin A D 2002 *Supercond. Sci. Technol.* **15** 1140
[25] Hardy V *et al* 2004 *Phys. Rev.* B **69** 020407
[26] Callister W D 2005 *Materials Science and Engineering* (New York: Wiley)
[27] Perkins G K *et al* 2007 *J. Phys.: Condens. Matter* **19** 176213